ACS chemical biology

Articles

pubs.acs.org/acschemicalbiology

Synthetic, Non-saccharide, Glycosaminoglycan Mimetics Selectively Target Colon Cancer Stem Cells

Nirmita J. Patel,[†] Rajesh Karuturi,[‡] Rami A. Al-Horani,[‡] Somesh Baranwal,[†,§] Jagrut Patel,[†] Umesh R. Desai,*[,‡] and Bhaumik B. Patel*[,†,§,∥]

[†]Hunter Holmes McGuire VA Medical Center, Richmond, Virginia 23249, United States

[‡]Department of Medicinal Chemistry and Institute for Structural Biology and Drug Discovery, Virginia Commonwealth University, Richmond, Virginia 23219, United States

[§]Division of Hematology, Oncology, and Palliative Care, Department of Internal Medicine and [∥]Massey Cancer Center, Virginia Commonwealth University, Richmond, Virginia 23298, United States

Supporting Information

ABSTRACT: Selective targeting of cancer stem-like cells (CSCs) is a paradigm-shifting approach. We hypothesized that CSCs can be targeted by interfering with functions of sulfated glycosaminoglycans, which play key roles in cancer cell growth, invasion and metastasis. We developed a tandem, dual screen strategy involving (1) assessing inhibition of monolayer versus spheroid growth and (2) assessing inhibition of primary versus secondary spheroid growth to identify G2.2, a unique sulfated nonsaccharide GAG mimetic (NSGM) from a focused library of 53 molecules, as a selective inhibitor of colon CSCs.

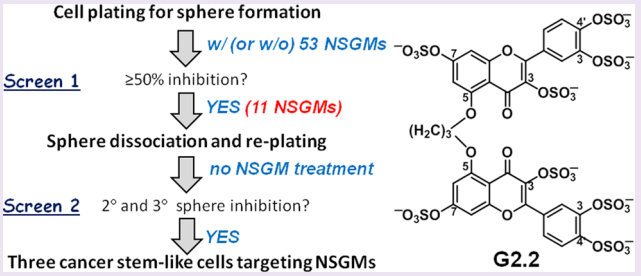

The NSGM down-regulated several CSC markers through regulation of gene transcription, while closely related, inactive NSGMs G1.4 and G4.1 demonstrated no such changes. G2.2's effects on CSCs were mediated, in part, through induction of apoptosis and inhibition of self-renewal factors. Overall, this work presents the proof-of-principle that CSCs can be selectively targeted through novel NSGMs, which are likely to advance fundamental understanding on CSCs while also aiding development of novel therapeutic agents.

The cancer stem-like cell (CSC) hypothesis has attracted attention as a unifying hypothesis that explains disease recurrence in the majority of advanced epithelial malignancies including colorectal cancer. CSCs typically survive anticancer drug treatment and self-renew to eventually reconstitute the entire tumor.[1−4] The recurrence of tumor is difficult to treat with traditional anticancer drugs that primarily target "bulk" cancer cells. A new approach is critically needed to prevent disease recurrence arising from inability to destroy CSCs.

Small molecule inhibition of CSC self-renewal to eventually eradicate tumor is a paradigm-shifting approach and presents major opportunity for discovering of novel anticancer drugs. Yet, selective targeting of CSC is challenging. CSCs are rare in a tumor cell population, which implies that approaches relying on screening of bulk cancer cells cannot succeed in identifying CSC-specific agents. Gupta et al. used epithelial−mesenchymal transition in a breast cancer cell line to enhance the proportion of CSCs, which enabled a high-throughput screening approach. This effort led to the identification of salinomycin as a CSC inhibitor.[5] This approach was also used recently by the NIH Molecular Libraries Program to identify several probes, for example, ML239, ML243, and ML245, as inhibitors of breast CSCs.[6−8]

We reasoned that a novel approach to target CSCs would be modulation of glycosaminoglycan (GAG) interactions with growth factors, cytokines, or morphogens that play critical roles in CSC growth and/or differentiation.[3,9,10] Heparan sulfate (HS), a sulfated GAG, is a recognized regulator of stem cell growth.[11] HS and its sulfation level is also known to induce stem cell differentiation.[12−14] Although the exact molecular mechanism of HS action on stem cells remains unelucidated, one postulate is that HS facilitates ternary complexation with cell surface proteins, thereby affecting growth and/or differentation.[11] This ternary complexation is likely to depend on HS fine structure, which presents a major opportunity for developing highly selective therapeutic strategies. Likewise, a chondroitin sulfate (CS)−containing proteoglycan called CSPG4 is also present on CSCs and is involved in regulating cell proliferation, migration, and angiogenesis.[15]

Although HS and CS play major roles in growth and differentiation of CSCs, they also contribute to bulk tumor cell biology.[3] This implies selective targeting of CSCs through GAG modulation can be expected to be difficult from the perspective of competing GAG modulation of bulk tumor cells also. Yet, we posited that the significant difference in growth profiles of the

Received: January 6, 2014
Accepted: June 10, 2014
Published: June 10, 2014

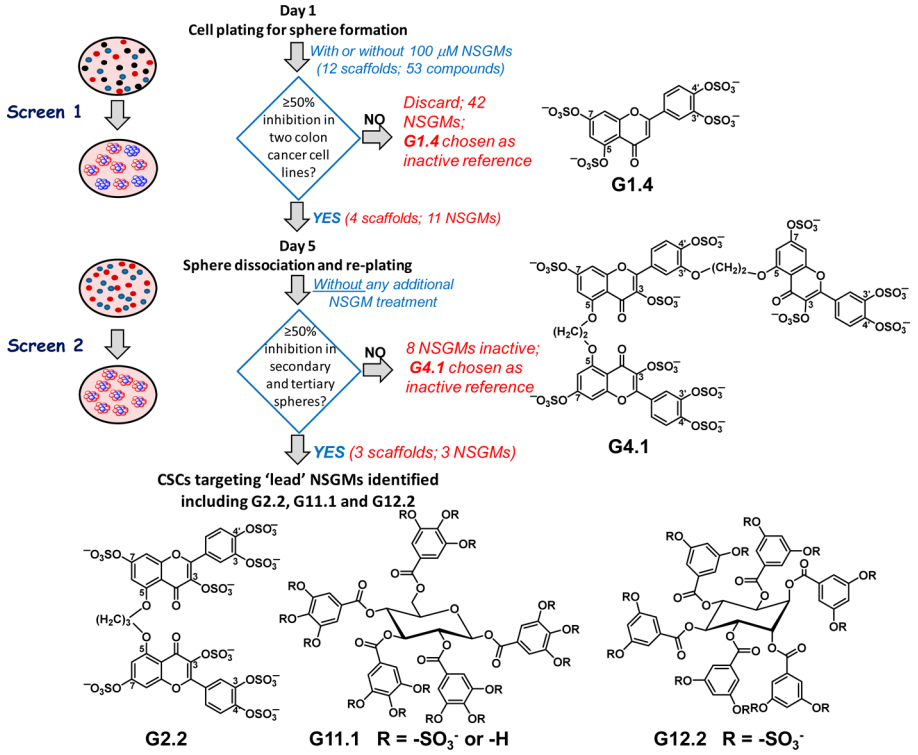

Figure 1. Selective targeting of colorectal cancer stem-like cells (CSCs) by tandem, dual screening of a focused sulfated NSGM library of 53 compounds belonging to 12 scaffolds (see Supporting Information Figures S1 and S2 for all structures). The protocol involved differential screening analysis of CSC growth under monolayer versus spheroid conditions (labeled "Screen 1") followed by primary versus secondary/tertiary growth ("Screen 2"). The screen identified three "lead" NSGMs, of which G2.2 was especially interesting because its two closely related analogues G1.4 and G4.1 were found to be inactive following screen 1 and screen 2, respectively. All 53 NSGMs were screened at 100 μM concentration.

two types of cells should enable a selective targeting strategy. This reasoning is supported in part by the differential expression of signaling pathway components of the two types of cells.[10,16] Further, recent evidence indicates that certain glycans may be aberrantly expressed in CSCs.[17] Thus, we hypothesized that intercepting appropriate GAG−protein interaction(s) may lead to selective targeting of CSCs.

Recently, we developed a range of structurally unique, synthetic nonsaccharide GAG mimetics (NSGMs, see Supporting Information Figures S1 and S2 for structures).[18,19] These novel molecules mimic GAG structure through appropriate placement of one or more sulfate group(s) on an aromatic scaffold. These NSGMs have been found to modulate several biological functions including coagulation, angiogenesis, inflammation, and oxidation in which GAGs play important roles.[18] Thus, if a biological screen can be designed to exploit the difference(s) in growth characteristics between bulk cancer cells and CSCs, then novel synthetic NSGMs that selectively target CSCs should be possible to identify.

Herein, we report that screening a library of 53 novel, synthetic, and homogeneous NSGMs containing varying levels of sulfation and diverse aromatic scaffolds resulted in identification of three NSGMs (i.e., G2.2, G11.1, and G12.2) that selectively inhibit the growth and self-renewal properties of colorectal CSCs (Figure 1). The CSC inhibition activity was highly sensitive to the structure of the NSGM. For example, closely related analogues, G1.4 and G4.1, do not induce CSC inhibition. In the process, we have developed a novel tandem, dual screening strategy involving inhibition of monolayer versus spheroid growth and inhibition of primary (1°) versus secondary (2°) spheroid growth that can be very broadly applied for anticancer chemical biology and drug discovery. The identified NSGM down-regulated several CSC markers through regulation of gene transcription, while closely related, inactive NSGMs demonstrated no such changes. Moreover, the effects on CSCs were mediated, in part, through induction of apoptosis and inhibition of self-renewal factors. Thus, our work presents the paradigm that NSGMs (and GAGs) represent a rich, untapped avenue for modulation of CSCs.

RESULTS AND DISCUSSION

Rationale, Design, and Synthesis of Non-saccharide GAG Mimetics Library. Structurally, GAGs are polymers of alternating hexosamine and hexuronic acid residues that are variably sulfated resulting in a natural library of millions of sequences. The core polysaccharide scaffold primarily orients key sulfate groups in three-dimensional space for optimal interaction with the target protein.[18,20] Sulfated NSGMs attempt to exploit this concept of functional mimicry through sulfate group recognition. In fact, this concept has led to the design of sulfated flavonoids[20,21] and sulfated tetrahydroisoquinolines[22] as mimetics of a specific sequence in heparin using computational techniques. Likewise, sulfated quinazolinones,[23] sulfated benzofurans,[24] and sulfated gallolylglucopyranoses[25] have also been developed as effective mimetics of GAGs. These small, synthetic, homogeneous molecules bind in the GAG-binding site of proteins resulting in modulation of function.[20−25] This function could be either agonistic or antagonistic. For example, sulfated tetrahydroisoquinolines mimic the interaction of heparin with antithrombin and thereby generate agonistic effect.[22] In contrast, sulfated

dx.doi.org/10.1021/cb500402f | ACS Chem. Biol. 2014, 9, 1826−1833

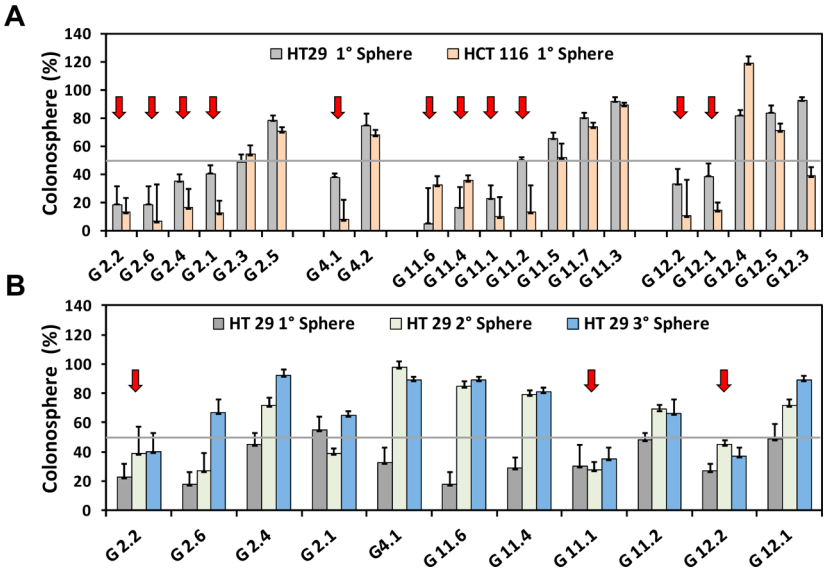

Figure 2. Results of the tandem, dual screening strategy. (A) Screen 1 results following primary spheroid growth studies in two colon cancer cell lines HCT-116 (p53 wild type, K-RAS mutant, microsatellite instable) and HT-29 (p53 mutant, K-RAS wild type, microsatellite stable). The 20 NSGMs identified for this study were at 100 μM concentration. (B) Screen 2 (secondary (2°) and tertiary (3°) growth assays) results with hits identified in Screen 1. Note: NSGMs were not added to the medium in 2° and 3° growth assays. Red arrows indicate positive hits in Screen 1 (A) and Screen 2 (B) ($p < 0.0005$). Data is represented as percent of vehicle-treated cells. Error bars represent ±1 SEM.

benzofurans introduce hydrophobic as well as electrostatic interactions and result in an antagonistic effect.[24]

Taking into account the role of GAGs in CSC growth and differentiation, we predicted that a distinct NSGM may selectively target colorectal CSCs. Hence, a small library of sulfated NSGMs was selected for screening (see Supporting Information Figures S1 and S2). As a group, the library represented 12 distinct scaffolds, G1 through G12, and 53 unique molecules possessing one to 13 sulfate groups, linear length of ∼8−24 Å and a range of three-dimensional shape from approximately planar (G1 scaffold) to globular (G12). Except for the G2−G4, G11 and G12 scaffolds, the synthesis of other scaffolds has been reported.[19−25] We report here the synthesis of G2−G4 NSGMs (see Supporting Information Schemes S1−S3). The synthesis of these molecules exploited the differential reactivity of the 5- and 3′-phenolic groups present on quercetin arising from the differential intramolecular hydrogen bonding. The differentially protected quercetins could then be site-selectively coupled to afford either G2 (5−5 coupling) or G3 mimetics (3′−3′ coupling) in high yields. Extension of this technique further led to the synthesis of G4 group of NSGMs by coupling G2 with the G1 scaffold. The final step is sulfation of the polyphenolic precursor using trialkylamine−sulfur trioxide complex under microwave conditions[26] (Supporting Information Schemes S4−S8). It is important to note that the synthetic strategy developed here provides novel variably sulfated molecules in high yields and high homogeneity (>95% purity).

Identification of Sulfated NSGMs that Inhibit Growth and Self-Renewal of CSCs. To study the CSC-targeting ability of the sulfated NSGMs, we utilized our earlier observation that CSCs/progenitors are enhanced several-fold in spheroid culture compared to monolayer culture.[27] In fact, colon HT-29 spheroids were found to express Leu-rich repeat-containing G-protein coupled receptor 5 (LGR5), an established CSC marker,[28] several-fold higher than cells grown as monolayers (Supporting Information Figure S3). More importantly, CSCs grown in spheroid condition differ significantly from monolayer counterparts with respect to activation of key signaling pathways, for example, Wnt/β-catenin signaling among others.[16,27] We exploited this to develop a novel screen for identifying molecules that selectively target colorectal CSCs. In this screen, sulfated NSGMs that inhibit HT-29 growth under spheroid conditions, but not under monolayer conditions, were then assessed for retention of 2° and 3° spheroid growth inhibition profiles in the absence of NSGM. The latter screen is of particular importance as primary spheroid growth although selective for CSCs doses not distinguish between non-self-renewing progenitors and self-renewing CSCs. Hence, sulfated NSGMs that satisfy this tandem, dual screen would preferentially target self-renewing CSCs. From the library of 53 sulfated NSGMs, 11 showed >50% inhibition of primary sphere formation in HT-29 cells (Figure 2) without inducing any meaningful inhibition of monolayer growth (see Supporting Information Figure S4 for all results). These 11 NSGMs belonged to G2, G4, G11, and G12 scaffolds but only four of the six G2 molecules, one of the two G4, four of the seven G11 and two of the five G12 molecules satisfied the first screen. Similar results were observed for HCT-116 colon cancer cell line (Figure 2a), which has a distinct genetic background compared to HT-29 cells. Interestingly, the active G2 and G4 NSGMs showed better inhibition of HCT-116 CSCs (p53 wild-type) as compared to HT-29 spheroids (p53 mutant). In contrast, G11 and G12 NSGMs did not display such a consistent trend.

The 11 sulfated NSGMs were then studied for their effect on 2° and 3° sphere formation (HT-29 and HCT-116) in Screen 2. By design, this screen reflects a test of true self-renewability of CSCs.[2,3] Single cell suspension obtained from primary spheres formed above was then cultured in the absence of NSGM. Only three (G2.2, G11.1 and G12.2) showed >50% inhibition in both 2° and 3° sphere formation in HT-29 cells (Figure 2b). Of these three, G2.2 (a dimeric sulfated flavonoid) was especially interesting because two closely related analogues,

dx.doi.org/10.1021/cb500402f | ACS Chem. Biol. 2014, 9, 1826−1833

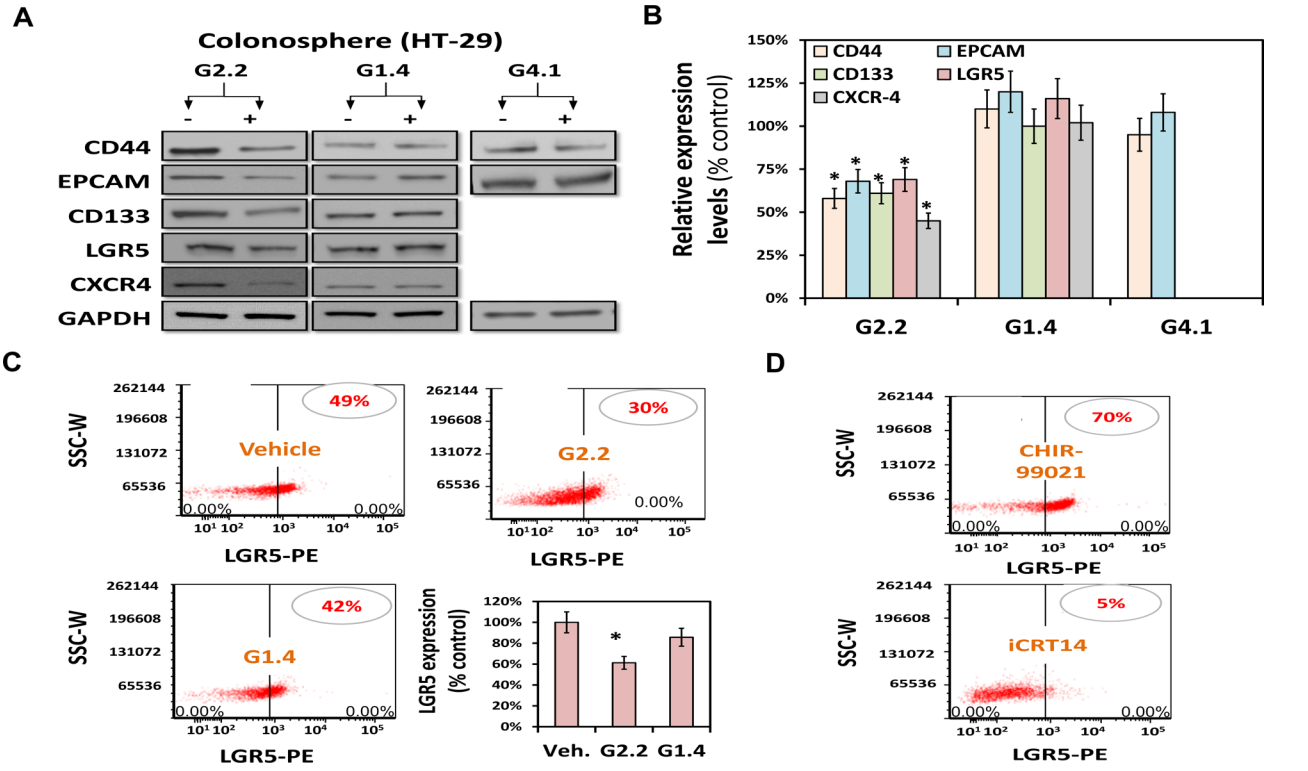

Figure 3. Effects of G2.2 and its inactive structural analogues, G1.4 and G4.1, on CSC markers. (A and B) shows the effect on the protein expression of CSC markers including CD44, EpCAM, CD133, LGR5, and CXCR4, while (C) shows flow cytometry profiles of LGR5, a CSC marker, expression in spheroids treated with G2.2 (100 μM) or its analogues (100 μM) as compared to vehicle-treated cells. (D) shows the results of treatment with known pharmacological activator (GSK-3β inhibitor, CHIR-99021(100 nM)) and inhibitor (iCRT14 (40 nM)) of β-catenin pathway, which regulates LGR5 expression, were used as biological control to establish appropriate gating for analyses of flow data (C). Western blots (A) were performed using antibodies available for the studied CSC markers. GAPDH is the house-keeping control. Bar graphs (B) show the relative change in expression levels of the marker in comparison to vehicle-treated CSCs using densitometry. Error bars represent ±1 SEM *represents $p <$ 0.01 compared to respective controls.

G1.4 (monomeric) and G4.1 (trimeric), completely failed at Screen 1 and Screen 2 stages, respectively (Figure 1). G2.2, the "lead" NSGM demonstrated a steep dose−response profile for primary spheroid inhibition with an apparent IC_{50} of ∼58 μM (Supporting Information Figure S5). Moreover, G2.2 also inhibited spheroid formation in HCT-116 (p53 null) and Panc-1 (pancreatic) cancer cell lines with essentially identical potency (Supporting Information Figure S6). The results suggested a more generic applicability of CSC-targeting effect of G2.2.

G2.2 Induces Distinct Molecular Changes Supporting Phenotypic Effects. As predicted on the basis of results achieved in the selective targeting assay, G2.2 inhibited expression of CSCs markers and self-renewal factors in HT-29 colon cancer cells confirming its CSC-targeting ability. G2.2 reduced the expression of all five CSCs markers[28,29] examined including CD44, CD133, epithelial adhesion molecule (EpCAM), LGR5, C-X-C chemokine receptor type 4 (CXCR-4) by ∼25−55% (Figure 3a and b). In striking contrast, G1.4 and G4.1 displayed no effect on the expression of any of the CSCs markers tested (Figure 3a and b). Additionally, flow-cytometric analyses for LGR5 showed a similar (39%) reduction in LGR5 (hi) cells following treatment with G2.2, but only a modest (<15%) decrease with G1.4 compared to vehicle-treated controls (Figure 3c). To confirm that these changes are meaningful, we performed two control experiments with agents known to up- or down-regulate LGR5. Considering that LGR5 is a target of canonical β-catenin signaling,[30] exposure to an activator (GSK-3β inhibitor CHIR-99021)[31] or inhibitor (iCRT14)[32] of β-catenin signaling should predictably alter expression of LGR5. Figure 3d results confirm these predictions and further support the phenotypic changes induced by G2.2. Likewise, similar findings were observed for DCLK1, another intestinal stem cell marker that is highly expressed in colon CSCs[33] (see Supporting Information Figure S7).

To understand the mechanism by which G2.2 might induce these molecular changes, we examined expression of above CSC markers at mRNA and protein levels at various time points. We observed a marked decrease in mRNA levels of several CSC markers at 6 h following treatment with G2.2 compared to controls (Figure 4a). With regard to the corresponding proteins, there was minimal change at 6 h but a significant decrease at 24 h (Figure 4b). These findings suggest that mRNA changes precede changes in protein expression strongly supporting the notion that G2.2 regulates CSC markers through regulation of gene transcription. Taken together, these results provide compelling evidence that G2.2 targets CSCs at a molecular level, which supports the phenotypic findings of spheroid growth inhibition described above. More importantly, the structure−activity dependence observed between two related NSGMs suggest that the fine structure of the molecule is critical for the CSC targeting ability.

Mechanism of G2.2 Mediated Inhibition of CSC Growth. To gain further insight into mechanism of selective CSC targeting by G2.2, we examined its effect on broad cellular

dx.doi.org/10.1021/cb500402f | ACS Chem. Biol. 2014, 9, 1826−1833

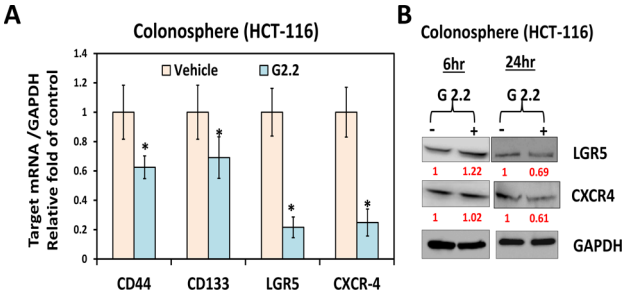

Figure 4. Effects of G2.2 on the mRNA levels of CSC markers at 6 h (A). Real-time quantitative reverse transcriptase polymerase chain reaction was used to determine relative mRNA expression of CSC genes and GAPDH served as house-keeping control. (B) shows the protein expression of select CSC markers LGR5 and CXCR4 at 6- and 24 h following treatment with G2.2 (100 μM) or vehicle. Numbers under the blot in red (B) show the relative change in expression levels of the marker in comparison to vehicle-treated CSCs using densitometry. Error bars represent ±1 SEM; * represents $p < 0.01$ compared to respective controls.

processes in spheroid cells. CSC growth is regulated by a fine balance between self-renewal and differentiation.[34] We examined CK20, a marker of colonic differentiation, expression in spheroid cells grown on collagen in the presence of 2.5% serum, which is known to promote differentiation,[16] following treatment with G2.2. We observed only a modest induction of CK20 expression following G2.2 treatment compared to vehicle treated controls using two different methods (Western blot and immunocytochemistry, Figures 5a and b). On the other hand, G2.2 caused a significant inhibition of self-renewal factors BMI-1 and c-MYC, while it had little effect on OCT-4 levels (Figures 5c and d). In comparison, the inactive analogue G1.4 induced no such changes (Figures 5c and d). These findings suggest that G2.2 might inhibit CSC growth, at least in part, through

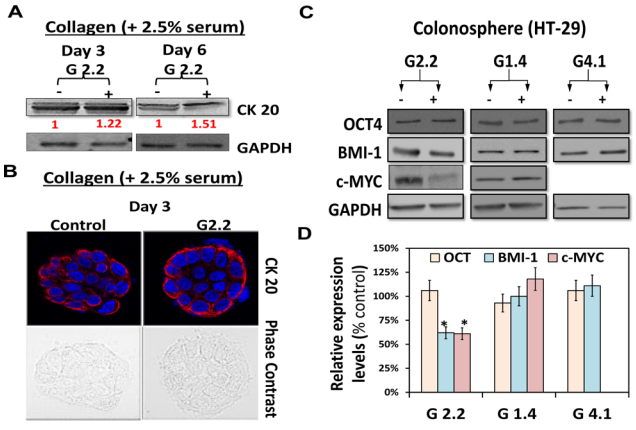

Figure 5. Mechanisms of CSC targeting by G2.2. (A, B) Expression of colonic differentiation marker CK20 in colonosphere cells at various time points using Western-blot (A) and immunocytochemistry and imaged with confocal microscopy (B). Differentiation was induced by growing the cells on collagen matrix in the presence of 2.5% serum. (C, D) The effect on the expression of self-renewal factors including OCT4, BMI-1 and C-MYC. Bar graphs (D) show the relative change in expression levels of the marker in comparison to vehicle-treated CSCs using densitometry. NSGM treatment was carried out at 100 μM concentration. Error bars represent ±1 SEM; * represents $p < 0.01$ compared to respective controls. The experiments were carried out in HT-29 colon cancer cells.

attenuation of self-renewal. In fact, inhibition of BMI-1 expression in colon cancer is being currently exploited as a therapeutic strategy to selectively target CSCs.[35]

To understand if G2.2 might exert additional effects on growth/survival of CSCs, we examined cell cycle distribution as well as induction of apoptosis in spheroid cells. G2.2 caused a very modest effect on cell cycle progression as evident by the small increase in proportion of spheroid cells in G1 phase compared to vehicle treated controls (Figure 6). On the other

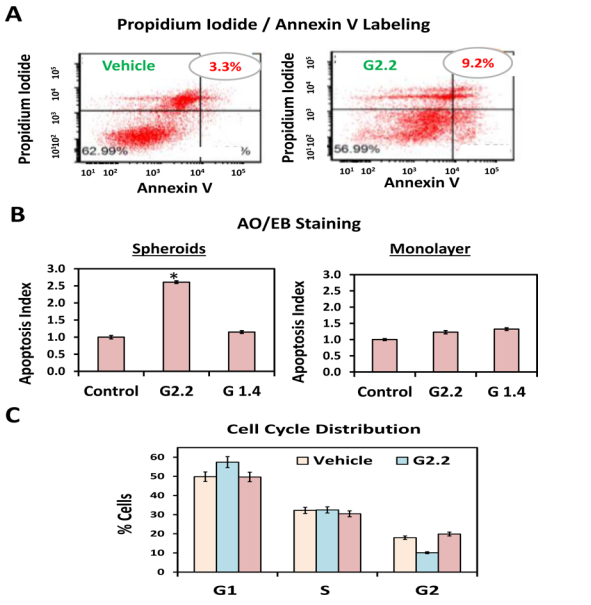

Figure 6. Mechanisms of CSC targeting by G2.2. (A, B) Apoptosis induction was measured as proportion of annexin V (+)/propidium iodide (+) cells (A) and as relative proportion of cells exhibiting nuclear changes characteristic of apoptosis using fluorescence microscopy following staining with acridine orange and ethidium bromide dyes (B). Apoptosis index = ([apoptotic cells (exp.)/total cells (exp.)]/[apoptotic cells (ctr.)/total cells (ctr.)]). (C) Shows relative cell cycle distribution at 24 h following appropriate treatment. Treatment with respective NSGM (100 μM) was carried out in HT-29 colon cancer cells. Error bars represent ±1 SEM; * represents $p < 0.01$ compared to respective controls.

hand, using two different methods to examine apoptosis induction, annexin V labeling and acridine orange/ethidium bromide staining, we observed a 2 to 3-fold induction of apoptosis in spheroid cells treated with G2.2 compared to vehicle treated controls (Figure 6a and b). In contrast, the inactive analogue G1.4 demonstrated no such effects (Figure 6b). Moreover, G2.2 did not induce apoptosis in CSC-poor monolayer counterparts (Figure 6b). Overall, the findings suggest that G2.2 selectively inhibits CSCs through induction of apoptosis as well as attenuation of self-renewal.

Conclusions. This is the first report describing anticolon CSC selective properties of a NSGM. These molecules represent a major translational advance over naturally occurring GAGs because of their ease of synthesis, biophysical properties (hydrophobic as well as hydrophilic nature) and structural homogeneity.[18] In fact, the structural complexity of GAGs has been a major challenge and NSGMs are likely to fulfill the major gap in availability of GAG-like molecules.

The therapeutic and chemical biology potential of NSGMs and GAG-like molecules is high. PI-88, a mixture of highly sulfated oligomannans that targets growth factor signaling, is

dx.doi.org/10.1021/cb500402f | ACS Chem. Biol. 2014, 9, 1826−1833

being currently evaluated in clinical trials of various cancers.[36,37] However, it is not known whether PI-88 targets CSCs. NSGMs also possesses multiple sulfate groups, in the manner of PI-88, and our earlier work shows that they typically bind in the GAG-binding site on proteins and modulate function.[18−23] The fine structure−activity relationship noted in the anti-CSC function of NSGMs suggests recognition of one or more target protein(s). Identification of these proteins should facilitate the design of more potent analogues. One important finding of this work is that G2.2 inhibits CSCs from several cell lines (HT-29, HCT-116 and Panc-1). This implies that a broader anti-CSC profile is possible through NSGMs, which should enhance the clinical relevance of these novel molecules.

Finally, our tandem, dual screen approach opens up a novel and relatively simple avenue for not only discovering anti-CSC agents but also identifying agents selectively targeting progenitor cells. In fact, we discuss such an observation with G4.1. Although G4.1 belongs to the same core scaffold as G2.2 (the flavonoid scaffold), it exerts its effects mostly on early progenitor cells. This finding implies that microscopic configurational and/or conformational differences play key roles in fine-tuning selectivity for targeting CSCs or progenitor cells. Such structural dependence of biological activity for NSGMs has been observed earlier and highlights the possibility of using this approach for advancing fundamental functional understating of stem cells/progenitors biology using chemical tools.

MATERIALS AND METHODS

Chemicals, Reagents, and Chemical Methods. Anhydrous CH_2Cl_2, THF, CH_3CN, DMF, methanol, acetone. and HPLC grade solvents were purchased from Sigma-Aldrich or Fisher and used as such. All other chemicals were of reaction grade as used as received from Sigma-Aldrich, Fisher, or TCI America. *n*-Hexylamine for ion-pairing UPLC was from Acros Organics. Analytical TLC was performed using UNIPLATE silica gel GHLF 250 um precoated plates (ANALTECH). Column chromatography was performed using silica gel (200−400 mesh, 60 Å) from Sigma-Aldrich. Flash chromatography was performed using Teledyne ISCO, Combiflash RF system and disposable normal silica cartridges of 30−50 μ particle size, 230−400 mesh size, and 60 Å pore size. Sulfated molecules were purified using Sephadex G10 size exclusion chromatography. The quaternary ammonium counterion of sulfate groups present in the molecules was exchanged for sodium ion using SP Sephadex−Na cation exchange chromatography. Each compound was characterized using ^{1}H and ^{13}C NMR spectroscopy, which was performed on Bruker 400 MHz spectrometer in either $CDCl_3$, CD_3OD, acetone-d_6, or D_2O. ESI MS of unsulfated molecules were recorded using Waters Acquity TQD MS spectrometer in positive ion mode, whereas ESI MS negative mode was used for sulfated compounds.

Synthesis and Characterization of Non-Saccharide Glycosaminoglycan Mimetics (NSGMs). The synthesis of G1.1−G1.7, G5.1−G5.2, G6.1−6.11, G7.1, G8.1, G9.1−9.2, G10.1−G10.8, and G11.1 has been reported earlier[19−25] and hence not presented here. NSGMs belonging to the G2, G3, G4, G11 (except for G11.1), and G12 scaffolds are new and are being reported for the first time. The detailed synthesis of these NSGMs (and intermediates used in their synthesis) is described in Schemes S1 through S8 in the online Supporting Information section. The synthetic protocol involves several steps of traditional organic chemistry transformations that typically yield good yields. Each new compound was characterized using ^{1}H and ^{13}C NMR spectroscopies on Bruker 400 MHz spectrometer and ESI-MS using Waters Acquity TQD MS spectrometer. The spectral data for newly synthesized molecules are presented in the online Supporting Information.

Cell Culture. HT-29 and HCT-116 human colon cancer cells were kindly gifted by Dr. Majumdar (Wayne State University) and PANC-1 cells were obtained from ATCC. These cells were maintained in 10 cm tissue cultured treated plate (USA Scientific) as monolayer in Dulbecco's Modified Eagle Medium: Nutrient Mixture F-12 (DMEM/F-12) (Gibco) supplemented with 10% fetal bovine serum (FBS) (Gibco), and 1% streptomycin/penicillin(AA) (Gibco). The cells were passaged using trypsin containing ethylenediaminetraacetic acid (EDTA) (Gibco) before they reached 70% confluence.

Cell Proliferation Assay. Cell proliferation was evaluated by (3-(4,5-dimethylthiazol-2-yl)-2,5-diphenyltetrazolium bromide) MTT cell proliferation assay. For HT-29 cell line approximately 2.5×10^3 cells/100 μL/well were plated in 96-well tissue culture treated plate. After overnight incubation at 37 °C vehicle (control) or NSGM was added at the desired concentration and the cells were further incubated for 60−72 h. At the end of the incubation, 10 μL of 5 mg mL^{-1} MTT solution (Sigma) made in phosphate buffered saline (PBS) (Gibco) was added to each well and incubated for minimum of 2 to 3 h until crystals formation was observed. Following this, 150 μL of 4 mM HCl (Sigma) in isopropanol solution was added dropwise to each well and the mixture was triturated until the crystals dissolve completely. Finally, the plate was placed on the spectrophotometer reader and read at 590 nm and growth inhibition was calculated as percent of control.

Primary (1°) Colonosphere Formation Assay. For primary sphere formation, cells were plated in nontreated, low adhesion, 96 wells plate at the concentration of 100 cells/100 μL/well in stem cell media (SCM) that consisted of DMEM:F12:AA (Gibco), supplemented with 1× B27 (Gibco), 20 ng/mL epidermal growth factor, and 10 ng/mL fibroblast growth factor (Sigma). After 4 h of incubation, vehicle (control) or NSGM at the desired concentrations were added to each well (at least in triplicates for each sample). On day five, numbers of spheres ranging from 50 to 150 mm in diameter were counted using phase contrast microscope and percent inhibition was calculated compared to control.

Secondary (2°) and Tertiary (3°) Colonosphere Assay. For secondary colonospheres, the 96-well plate of primary spheres was centrifuged at speed of 1000 rpm for 1 min and the supernatant was removed. Spheres that settled at the base of the plate were trypsinized with 20 μL/well and single cell suspension was prepared using vigorous mechanical dissociation. The numbers of viable cell were counted with 1:5 ratio of cell: trypan blue and then replated at 100 cells/100 mL/well in SCM media in a low adhesion plate. No further treatment with NSGMs was performed. Numbers of spheres were counted as above on day 5. The same method was repeated for tertiary spheres.

Western Blotting Analysis. Western blot analysis was performed according to the standard protocol described in the literature. Briefly, HT-29 cells were plated in serum-free SCM in a low adhesion 6-well plate to obtain spheroids. Mature spheroids were treated on day 4 after plating, with vehicle or NSGMs for indicated time and cells were solubilized in lysis buffer (20 mM Na_3PO_4, 100 mM NaCl, 2 mM EDTA, 1% Nonidet P-40, 2.5 mM Na_3VO_4) containing protease (Roche) as well as phosphatase inhibitor cocktails (Sigma). Following centrifugation at 14 000 g for 15 min, the supernatant was used for Western blot analysis. In all analyses, protein concentration was determined by the Bio-Rad Protein Assay kit (Bio-Rad). Approximately 25−50 μg of protein was separated by polyacrylamide gel electrophoresis and was transferred to PVDF membrane (Bio-Rad). Blocking was done with 5% low fat milk powder for 1 h followed by overnight incubation with primary antibody (dilution 1:1000): anti-CD44 (Cell Signaling), anti-EpCAM (Cell Signaling), anti-LGR5 (Origene), anti-CD133 ((Miltenyi Biotec), anti-CXCR4 (Abcam), anti-OCT4 (Cell Signaling), anti-BMI-1(Millipore), anti-c-MYC (Millipore), and anti-CK20 (Abcam). This was followed by incubation with appropriate secondary antibody and protein bands were visualized using the enhanced chemiluminescence detection system and imaged with LAS-3000 Imaging System (FUJIFILM). Densitometry was determined by AIDA image analyzer software (Raytest) and results were calculated as relative intensity compared to control. All experiments were performed at least three times.

Flow Cytometry Analysis. Human colon cancer HT-29 cells, grown in spheroid or monolayer condition were treated with vehicle or

dx.doi.org/10.1021/cb500402f | ACS Chem. Biol. 2014, 9, 1826−1833

NSGMs for 24 h, were trypsinized and single cells were resuspended at 10^6 cells/mL in PBS buffer. Cells were incubated with fluorophore conjugated antibody for 30 min at 4 °C and washed once with PBS buffer prior to analysis. Following antibody and dilution were used: LGR5-PE) (Dilution 1:50, Origene), DCLK1(Dilution 1:33, Abcam). Cell sorting was performed using FACSAria II High-Speed Cell Sorter (BD Biosciences) and data were analyzed with FCS Express 4 Flow Cytometry software (De-Novo Software).

Real-time PCR Analysis. Total RNA was isolated using the mirVana miRNA Isolation Kit (Life technologies, Grand Island, NY). One μg total RNA was reverse transcribed using First-Strand cDNA Synthesis Kit using hexamer reverse primer (Affymetrix). Real time QPCR was performed using RT^2 SYBR Green qPCR Master mix (Qiagen) in a 7500 fast real time machine (Applied Biosystem). Relative expressions of mRNA were calculated using ΔΔCT methods using GAPDH as a loading control. Primers used in the study include CXCR4 (Forward 5′ ACT ACA CCG AGG AAA TGG GCT 3′, Reverse 5′ CCC ACA ATG CCA GTT A AG A AGA 3′); CD44 (Forward 5′ AGC AAC CAA GAG GCA AGA AA 3′, Reverse 5′ GTG TGG TTG AAA TGG TGC TG 3′); LGR5 (Forward 5′ CTC CCA GGT CTG GTG TGT TG 3′, Reverse 5′ GAG GTC TAG GTA GGA GGT GAA G 3′); CD133 (Forward 5′ GGA CCC ATT GGC ATT CTC 3′, Reverse 5′CAG GAC ACA GCA TAG AAT AAT C 3′); GAPDH (Forward 5′ TGT TGC CAT CAA TGA CCC CTT 3′, Reverse 5′CTC CAC GAC GTA CTC AGC G 3′).

Differentiation Assay. Single cell suspension from mature HT-29 colonosphere pretreated with vehicle or G2.2 for 24 h were plated on collagen coated glass coverslips or flasks in the presence of media supplemented with 2.5% FBS containing G2.2 or vehicle. At indicated time points, cells lysate was examined for CK-20 expression with western-blot as above. Alternatively, cells were fixed with 4% paraformaldehyde for 20 min at RT, permeabilized for 5 min in 0.5% Triton X-100 solution and blocked in PBS containing 1% BSA for 1 h prior to incubation with anti-CK-20 antibody (Abcam) for 2 h. Cells were then washed, incubated for 60 min with Alexa Fluor conjugate secondary antibodies, rinsed with blocking buffer and mounted on slides with DAPI containing ProLong Gold Antifade Reagent (Invitrogen). Fluorescently labeled cells were examined using a Zeiss LSM700 laser scanning confocal microscope (Zeiss Micro imaging Inc.). Alexa Flour 555 signals were imaged sequentially at 40× magnification in frame-interlaced mode to eliminate cross talk between channels.

Apoptosis Assay. Human colon cancer HCT-116 cells, grown in spheroid condition were treated with vehicle or NSGMs for 24 h. Following which cells were trypsinized and single cells were resuspended at 10^6 cells/mL in PBS buffer. Two different methods were used to assess apoptosis induction. In the first methods, cells were incubated with propidium iodide and Annexin V-APC (ebioscience) and flow cytometric analyses were performed as above. In the second method, fluorescence microscopy was employed to examine morphological changes suggestive of apoptosis following staining with 1:1 mixture of 100 μg/mL each of acridine orange (AO) and ethidium bromide (EB) prepared in PBS. Briefly, a small volume of cell suspension was mounted on a glass slide and incubated with 1 μL of AO/EB solution and mixed gently just prior to microscopy and quantification. At least 500 cells in 10−15 fields were examined in each sample using Nikon ECLIPSE E800 M fluorescence microscope using 20× objective. Results were quantitated as proportion of cells exhibiting characteristic apoptotic morphology normalized to vehicle treated controls. The data was expressed as apoptosis index = [([apoptotic cells (NSGMs)/total cells (NSGMs)]/[apoptotic cells (vehicle)/total cells (vehicle)]).

Statistical Analysis. All data are expressed as means ± SEM unless otherwise indicated. The results were analyzed using the unpaired, two-tailed Student's t test. $p < 0.01$ was designated as the level of significance unless specified otherwise.

■ ASSOCIATED CONTENT

Ⓢ Supporting Information

This material is available free of charge via the Internet at http://pubs.acs.org.

■ AUTHOR INFORMATION

Corresponding Authors

*Phone: 804-675-5000 Ext. 4309. Email: bpatel2@mcvh-vcu.edu.

*Phone: 804-828-7328. Email: urdesai@vcu.edu.

Author Contributions

N.J.P. performed library screening and mechanistic studies, analyzed the results and assisted in writing the manuscript; R.K. and R.A.A.H. synthesized library of compounds; S.B. performed mechanistic studies, J.P. assisted in library screening; U.R.D. and B.B.P. directed the project, analyzed the results and wrote the manuscript.

Funding

This work was supported by grants HL090586 and HL107152 from the National Institutes of Health to U.R.D., a VA Merit award to B.B.P. and a postdoctoral fellowship from the American Heart Association—Mid-Atlantic Affiliate to R.A.A.H.

Notes

The authors declare no competing financial interest.

■ ABBREVIATIONS

1°, primary; 2°, secondary; 3°, tertiary; CSCs, cancer stem-like cells; GAG, glycosaminoglycan; HS, heparan sulfate; NSGM, nonsaccharide GAG mimetic

■ REFERENCES

(1) Gangemi, R., Paleari, L., Orengo, A. M., Cesario, A., Chessa, L., Ferrini, S., and Russo, P. (2009) Cancer stem cells: A new paradigm for understanding tumor growth and progression and drug resistance. *Curr. Med. Chem. 16*, 1688−1703.

(2) Dontu, G., Abdallah, W. M., Foley, J. M., Jackson, K. W., Clarke, M. F., Kawamura, M. J., and Wicha, M. S. (2003) *In vitro* propagation and transcriptional profiling of human mammary stem/progenitor cells. *Genes Dev. 17*, 1253−1270.

(3) Reya, T., Morrison, S. J., Clarke, M. F., and Weissman, I. L. (2001) Stem cells, cancer, and cancer stem cells. *Nature 414*, 105−111.

(4) Scatena, R., Bottoni, P., Pontoglio, A., and Giardina, B. (2011) Cancer stem cells: The development of new cancer therapeutics. *Expert Opin. Biol. Ther. 11*, 875−892.

(5) Gupta, P. B., Onder, T. T., Jiang, G., Tao, K., Kuperwasser, C., Weinberg, R. A., and Lander, E. S. (2009) Identification of selective inhibitors of cancer stem cells by high-throughput screening. *Cell 138*, 645−659.

(6) Carmody, L., Germain, A., Morgan, B., VerPlank, L., Fernandez, C., Feng, Y., Perez, J., Dandapani, S., Munoz, B., Palmer, M., Lander, E. S., Gupta, P. B., and Schreiber, S. L. (2010−2011) Probe Reports from the NIH Molecular Libraries Program [Internet]. National Center for Biotechnology Information (US), Bethesda, MD. PMID: 23762939.

(7) Carmody, L. C., Germain, A. R., VerPlank, L., Nag, P. P., Muñoz, B., Perez, J. R., and Palmer, M. A. (2012) Phenotypic high-throughput screening elucidates target pathway in breast cancer stem cell-like cells. *J. Biomol. Screen. 17*, 1204−1210.

(8) Germain, A. R., Carmody, L. C., Nag, P. P., Morgan, B., Verplank, L., Fernandez, C., Donckele, E., Feng, Y., Perez, J. R., Dandapani, S., Palmer, M., Lander, E. S., Gupta, P. B., Schreiber, S. L., and Munoz, B. (2013) Cinnamides as selective small-molecule inhibitors of a cellular model of breast cancer stem cells. *Bioorg. Med. Chem. Lett. 23*, 1834−1838.

(9) Ailles, L. E., and Weissman, I. L. (2007) Cancer stem cells in solid tumors. *Curr. Opin. Biotechnol. 18*, 460−466.
(10) Reya, T., and Clevers, H. (2005) Wnt signaling in stem cells and cancer. *Nature 434*, 843−850.
(11) Kraushaar, D. C., Dalton, S., and Wang, L. (2013) Heparan sulfate: A key regulator of embryonic stem cell fate. *Biol. Chem. 394*, 741−751.
(12) Hirano, K., Sasaki, N., Ichimiya, T., Miura, T., Van Kuppevelt, T. H., and Nishihara, S. (2012) 3-O-sulfated heparan sulfate recognized by the antibody HS4C3 contribute to the differentiation of mouse embryonic stem cells via Fas signaling. *PLoS One 7*, e43440.
(13) Johnson, C. E., Crawford, B. E., Stavridis, M., Ten Dam, G., Wat, A. L., Rushton, G., Ward, C. M., Wilson, V., van Kuppevelt, T. H., Esko, J. D., Smith, A., Gallagher, J. T., and Merry, C. L. (2007) Essential alterations of heparan sulfate during the differentiation of embryonic stem cells to Sox1-enhanced green fluorescent protein-expressing neural progenitor cells. *Stem Cells 25*, 1913−1923.
(14) Nairn, A. V., Kinoshita-Toyoda, A., Toyoda, H., Xie, J., Harris, K., Dalton, S., Kulik, M., Pierce, J. M., Toida, T., Moremen, K. W., and Linhardt, R. J. (2007) Glycomics of proteoglycan biosynthesis in murine embryonic stem cell differentiation. *J. Proteome Res. 6*, 4374−4387.
(15) Campoli, M., Ferrone, S., and Wang, X. (2010) Functional and clinical relevance of chondroitin sulfate proteoglycan 4. *Adv. Cancer Res. 109*, 73−121.
(16) Lombardo, Y., Scopelliti, A., Cammareri, P., Todaro, M., Iovino, F., Ricci-Vitiani, L., Gulotta, G., Dieli, F., de Maria, R., and Stassi, G. (2011) Bone morphogenetic protein 4 induces differentiation of colorectal cancer stem cells and increases their response to chemotherapy in mice. *Gastroenterology 140*, 297−309.
(17) Battula, V. L., Shi, Y., Evans, K. W., Wang, R. Y., Spaeth, E. L., Jacamo, R. O., Guerra, R., Sahin, A. A., Marini, F. C., Hortobagyi, G., Mani, S. A., and Andreeff, M. (2012) Ganglioside GD2 identifies breast cancer stem cells and promotes tumorigenesis. *J. Clin. Invest. 122*, 2066−2078.
(18) Desai, U. R. (2013) The promise of sulfated synthetic small molecules as modulators of glycosaminoglycan function. *Future Med. Chem. 5*, 1363−1366.
(19) Raman, K., Karuturi, R., Swarup, V. P., Desai, U. R., and Kuberan, B. (2012) Discovery of novel sulfonated small molecules that inhibit vascular tube formation. *Bioorg. Med. Chem. Lett. 22*, 4467−4470.
(20) Al-Horani, R. A., Ponnusamy, P., Mehta, A. Y., Gailani, D., and Desai, U. R. (2013) Sulfated pentagalloylglucoside is a potent, allosteric, and selective inhibitor of factor XIa. *J. Med. Chem. 56*, 867−878.
(21) Karuturi, R., Al-Horani, R. A., Mehta, S. C., Gailani, D., and Desai, U. R. (2013) Discovery of allosteric modulators of factor XIa by targeting hydrophobic domains adjacent to its heparin-binding site. *J. Med. Chem. 56*, 2415−2428.
(22) Sidhu, P. S., Abdel Aziz, M. H., Sarkar, A., Mehta, A. Y., Zhou, Q., and Desai, U. R. (2013) Designing allosteric regulators of thrombin. Exosite 2 features multiple subsites that can be targeted by sulfated small molecules for inducing inhibition. *J. Med. Chem. 56*, 5059−5070.
(23) Gunnarsson, G. T., and Desai, U. R. (2002) Designing small, nonsugar activators of antithrombin using hydropathic interaction analyses. *J. Med. Chem. 45*, 1233−1243.
(24) Gunnarsson, G. T., and Desai, U. R. (2002) Interaction of designed sulfated flavanoids with antithrombin: Lessons on the design of organic activators. *J. Med. Chem. 45*, 4460−4470.
(25) Al-Horani, R. A., Liang, A., and Desai, U. R. (2011) Designing nonsaccharide, allosteric activators of antithrombin for accelerated inhibition of factor Xa. *J. Med. Chem. 54*, 6125−6138.
(26) Al-Horani, R. A., and Desai, U. R. (2010) Chemical sulfation of small molecules—Advances and challenges. *Tetrahedron 66*, 2907−2918.
(27) Kanwar, S. S., Yu, Y., Nautiyal, J., Patel, B. B., and Majumdar, A. P. (2010) The Wnt/beta-catenin pathway regulates growth and maintenance of colonospheres. *Mol. Cancer 9*, 212.
(28) Vaiopoulos, A. G., Kostakis, I. D., Koutsilieris, M., and Papavassiliou, A. G. (2012) Colorectal cancer stem cells. *Stem Cells 30*, 363−371.
(29) Hermann, P. C., Huber, S. L., Herrler, T., Aicher, A., Ellwart, J. W., Guba, M., Bruns, C. J., and Heeschen, C. (2007) Distinct populations of cancer stem cells determine tumor growth and metastatic activity in human pancreatic cancer. *Cell Stem Cell 1*, 313−323.
(30) Barker, N., Ridgway, R. A., van Es, J. H., van de Wetering, M., Begthel, H., van den Born, M., Danenberg, E., Clarke, A. R., Sansom, O. J., and Clevers, H. (2009) Crypt stem cells as the cells-of-origin of intestinal cancer. *Nature 457*, 608−611.
(31) Sanchez-Ripoll, Y., Bone, H. K., Owen, T., Guedes, A. M., Abranches, E., Kumpfmueller, B., Spriggs, R. V., Henrique, D., and Welham, M. J. (2013) Glycogen synthase kinase-3 inhibition enhances translation of pluripotency-associated transcription factors to contribute to maintenance of mouse embryonic stem cell self-renewal. *PLoS One 8*, e60148.
(32) Gonsalves, F. C., Klein, K., Carson, B. B., Katz, S., Ekas, L. A., Evans, S., Nagourney, R., Cardozo, T., Brown, A. M., and DasGupta, R. (2011) An RNAi-based chemical genetic screen identifies three small-molecule inhibitors of the Wnt/wingless signaling pathway. *Proc. Natl. Acad. Sci. U.S.A. 108*, 5954−5963.
(33) Nakanishi, Y., Seno, H., Fukuoka, A., Ueo, T., Yamaga, Y., Maruno, T., Nakanishi, N., Kanda, K., Komekado, H., Kawada, M., Isomura, A., Kawada, K., Sakai, Y., Yanagita, M., Kageyama, R., Kawaguchi, Y., Taketo, M. M., Yonehara, S., and Chiba, T. (2013) Dclk1 distinguishes between tumor and normal stem cells in the intestine. *Nat. Genet. 45*, 98−103.
(34) Prasetyanti, P. R., Zimberlin, C. D., Bots, M., Vermeulen, L., Melo Fde, S., and Medema, J. P. (2013) Regulation of stem cell self-renewal and differentiation by Wnt and Notch are conserved throughout the adenoma-carcinoma sequence in the colon. *Mol. Cancer 12*, 126.
(35) Kreso, A., van Galen, P., Pedley, N. M., Lima-Fernandes, E., Frelin, C., Davis, T., Cao, L., Baiazitov, R., Du, W., Sydorenko, N., Moon, Y. C., Gibson, L., Wang, Y., Leung, C., Iscove, N. N., Arrowsmith, C. H., Szentgyorgyi, E., Gallinger, S., Dick, J. E., and O'Brien, C. A. (2014) Self-renewal as a therapeutic target in human colorectal cancer. *Nat. Med. 20*, 29−36.
(36) Ferro, V., Dredge, K., Liu, L., Hammond, E., Bytheway, I., Li, C., Johnstone, K., Karoli, T., Davis, K., Copeman, E., and Gautam, A. (2007) PI-88 and novel heparan sulfate mimetics inhibit angiogenesis. *Semin. Thromb. Hemost. 33*, 557−568.
(37) Lewis, K. D., Robinson, W. A., Millward, M. J., Powell, A., Price, J., Thomson, D. B., Walpole, E. T., Haydon, A. M., Creese, B. R., Roberts, K. L., Zalcberg, J. R., and Gonzalez, R. (2008) A phase II study of the heparanase inhibitor PI-88 in patients with advanced melanoma. *Invest. New Drugs 26*, 89−94.